

Communication: The electronic structure of matter probed with a single femtosecond hard x-ray pulse

J. Szlachetko,^{1,2,a)} C. J. Milne,¹ J. Hozowska,³ J.-Cl. Dousse,³
W. Błachucki,³ J. Sà,¹ Y. Kayser,¹ M. Messerschmidt,⁴ R. Abela,¹ S. Boutet,⁴
C. David,¹ G. Williams,⁴ M. Pajek,² B. D. Patterson,¹ G. Smolentsev,¹
J. A. van Bokhoven,^{1,5} and M. Nachtegaal^{1,b)}

¹Paul Scherrer Institute, Villigen, Switzerland

²Institute of Physics, Jan Kochanowski University, Kielce, Poland

³Department of Physics, University of Fribourg, Fribourg, Switzerland

⁴Linac Coherent Light Source (LCLS), SLAC National Accelerator Laboratory, Menlo Park, California 94025, USA

⁵Institute for Chemical and Bioengineering, ETH Zürich, Zürich, Switzerland

(Received 29 November 2013; accepted 28 February 2014; published online 17 March 2014)

Physical, biological, and chemical transformations are initiated by changes in the electronic configuration of the species involved. These electronic changes occur on the timescales of attoseconds (10^{-18} s) to femtoseconds (10^{-15} s) and drive all subsequent electronic reorganization as the system moves to a new equilibrium or quasi-equilibrium state. The ability to detect the dynamics of these electronic changes is crucial for understanding the potential energy surfaces upon which chemical and biological reactions take place. Here, we report on the determination of the electronic structure of matter using a single self-seeded femtosecond x-ray pulse from the Linac Coherent Light Source hard x-ray free electron laser. By measuring the high energy resolution off-resonant spectrum (HEROS), we were able to obtain information about the electronic density of states with a single femtosecond x-ray pulse. We show that the unoccupied electronic states of the scattering atom may be determined on a shot-to-shot basis and that the measured spectral shape is independent of the large intensity fluctuations of the incoming x-ray beam. Moreover, we demonstrate the chemical sensitivity and single-shot capability and limitations of HEROS, which enables the technique to track the electronic structural dynamics in matter on femtosecond time scales, making it an ideal probe technique for time-resolved X-ray experiments. © 2014 Author(s). All article content, except where otherwise noted, is licensed under a Creative Commons Attribution 3.0 Unported License. [<http://dx.doi.org/10.1063/1.4868260>]

The recent development of hard x-ray free electron lasers (XFELs) has resulted in the rapid development of research that takes advantage of the intense, femtosecond x-ray pulses generated by these facilities. XFELs have enabled the investigation of dynamic processes on the femtosecond timescale using x-ray techniques, they have introduced the ability to perform damage-free room temperature protein crystallography measurements, and they have opened the field of non-linear x-ray processes due to their enormous peak power as compared to other sources.¹⁻⁴

One of the more difficult techniques to apply at a free electron laser (FEL) has been x-ray absorption spectroscopy (XAS). The self-amplified stimulated emission (SASE) process, which generates the short x-ray pulses from the FEL, results in significant instability in both the number of photons generated per pulse, as well as in the photon energy.⁵ The result is a very unstable source of x-rays, with pulse-to-pulse intensity fluctuations of monochromatic x-rays of up to 100%.⁶ This introduces significant noise in any data that requires a series of sequential

^{a)}Electronic mail: jakub.szlachetko@psi.ch

^{b)}Electronic mail: maarten.nachtegaal@psi.ch

measurements to be performed; such as scanning the incident photon energy during an x-ray absorption scan or a resonant x-ray emission scan (RXES).^{7–9} Consequently, the ability to perform such measurements is entirely dependent on the precision with which the incoming x-ray flux can be measured. Until now, the only spectroscopic method that has proven to be insensitive to the XFEL pulse instabilities is x-ray emission spectroscopy (XES), where a dispersive spectrometer was used to obtain an XES spectrum on a shot-to-shot basis.^{10,11} XES gives access to the occupied electronic states and therefore provides only a partial picture of the electronic structure. To study intensity-induced X-ray transparency,¹² non-linear absorption mechanisms,¹³ or electron relaxation and rearrangement processes,¹⁴ it is crucial that information from both the occupied and unoccupied electronic states are to be measured.

XAS is the technique of choice to probe the unoccupied density of states. One possible XAS technique that allows a range of x-ray energies to be collected at once, partially avoiding the XFEL normalization problem, is dispersive XAS.^{15,16} The primary drawback of this technique at an XFEL is that in addition to the intensity fluctuations, the incident spectrum also shifts in photon energy. This technique thus requires both incident pulse energy normalization as well as incident spectrum normalization. The incident x-ray spectrum has been measured at Linac Coherent Light Source (LCLS) on a pulse-to-pulse basis, but the spectrometer used is not broadly tunable in energy, making it only effective over a narrow photon energy range.¹⁷ The second drawback to this approach is the narrow bandwidth of the XFEL, approximately 0.25%–0.5%,^{18–20} which restricts the range over which the XAS can be measured without requiring the incident photon energy to be scanned, something which is still non-trivial at an XFEL. However, very recent experiments have demonstrated the feasibility of dispersive XAS spectroscopy in transmission mode at the SACLA XFEL (SPring-8, Japan).²¹ High energy resolution off resonant spectroscopy (HEROS) allows measurement of a scattered X-ray spectrum in a single acquisition that represents the unoccupied density of states and is complementary to the ability of XES to probe the occupied density of states.^{22,23} HEROS has none of the drawbacks of dispersive XAS and can be used, as we demonstrate here, with a self-seeded XFEL beam to probe electronic states using single XFEL pulses.

The idea of using off-resonant excitations dates back to 1982 when, following the Kramers-Heisenberg relation,²⁴ Tulkki and Åberg developed simplified formulas to describe the second-order photon-atom interaction.²⁵ This theory is often used to calculate both the resonant and non-resonant x-ray emission spectra around the absorption edge of a scattering atom.^{26–29} In their original work, Tulkki and Åberg noticed that for incident beam energies tuned below an x-ray absorption edge (called the off-resonance region), the shape of the x-ray emission spectrum is proportional to the unoccupied density of states of an atom. However until recently, the potential of extracting the electronic structure from a single x-ray emission spectrum recorded at off-resonant excitations was not explored, likely due to the extremely weak scattering cross section as compared to the resonant x-ray emission spectrum.^{28,29} By combining off-resonant excitation and an x-ray spectrometer operating in a dispersive geometry at a synchrotron, HEROS has been experimentally demonstrated.^{22,23} HEROS is an alternative to XAS, with significant advantages when used with pulsed x-ray sources. By taking advantage of its ability to record an x-ray spectrum in a single measurement, it has been applied to monitoring the kinetics of a chemical reaction.²²

In this work, we explore the use of the HEROS technique to measure the electronic structure of copper and copper oxides at an XFEL. The experiment was performed at the Coherent X-ray Imaging instrument³⁰ at the Linac Coherent Light Source, USA. As reported previously^{22,23} HEROS requires monochromatic photon energies for the incoming beam. One approach to generating this type of beam at an XFEL is the so-called “self-seeding” method,³¹ which allows the FEL to produce a narrow energy bandwidth beam with more stable beam characteristics than during normal SASE operation with a monochromator.^{6,18} The experimental setup is schematically drawn in Figure 1. The x-rays delivered by the LCLS are generated by SASE and monochromatized to seed the electron beam in the second part of the undulator, imparting a suitable structure to the electron bunch to enable it to produce monochromatic pulses.^{18,31} However, because fine scanning of the seeded beam energy is not generally feasible

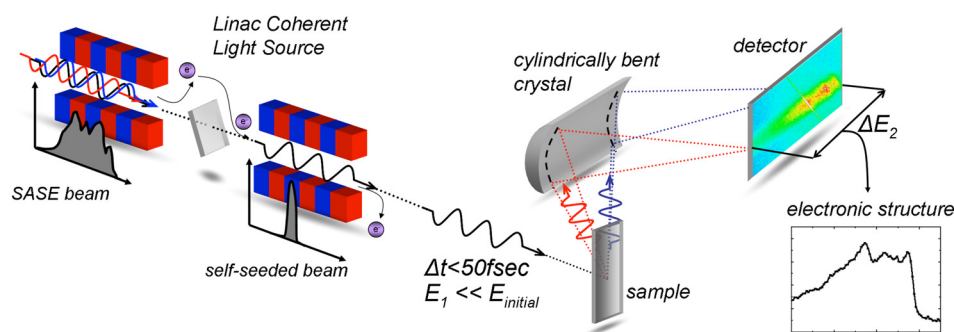


FIG. 1. Experimental setup for a high energy resolution off-resonant experiment at an x-ray free electron laser source. The first part of the LCLS undulator is used to generate sufficient X-ray energy through the SASE process, to generate a monochromatic seed pulse using a diamond crystal. This seed interacts with the electron beam and results in amplification of only a narrow energy bandwidth for the second part of the undulator. As a result monochromatic, 50 fs long x-ray pulses incident on the sample are obtained. The x-ray beam energy is tuned to below an absorption edge ($E_1 < E_{\text{initial}}$) to access the off-resonant excitations. The resulting x-ray fluorescence is recorded in dispersive mode by means of a von Hamos spectrometer consisting of a cylindrically bent crystal and a position sensitive detector.

at this point at XFELs, we could not perform comparative studies of HEROS and scanning-mode XAS during the experiment. For the present experiment, we used x-rays at an energy around the Cu K-absorption edge ($E_{\text{initial}} = 8979$ eV), and the energy bandwidth of the incoming beam was around 1.7 eV. The x-ray spot size on the sample was controlled by placing the sample away from the focus of the X-ray mirrors to produce a $10 \times 10 \mu\text{m}^2$ focal spot. A typical bright x-ray shot contained approximately $5\text{--}6 \times 10^{11}$ photons/pulse, corresponding to ~ 0.9 mJ. The LCLS machine was operated in high charge mode providing 50 fs long x-ray pulses at a repetition rate of 120 Hz. During the experiment we moved the sample continuously at a speed of 0.5 mm/s, and the analysis was performed only on well-seeded, spectrally narrow shots with a minimum spatial separation of $50 \mu\text{m}$ between measurements. For x-ray detection we employed a von Hamos type spectrometer operating at 25 cm radius of curvature.³² The use of a von Hamos x-ray emission spectrometer ensures that the measured spectra are of high energy resolution and can be collected without scanning any components. As a consequence, the ultimate acquisition time is limited only by the efficiency of the setup and the number of photons incident on the sample. The Cu x-ray fluorescence around $K\alpha_{1,2}$ was acquired using two segmented-type Si(444) crystals³² providing x-ray diffraction at Bragg angles of approximately 80° . Additionally, a Ge(800) crystal was employed at a Bragg angle of 80° to monitor the elastically scattered x-rays which provide information about the incoming x-ray energy and experimental resolution. The setup was aligned such that the diffracted x-rays were focused in three spatially separated spots onto the two 140 K CSPAD detectors³³ used to measure the scattered spectra. With the present setup, we could cover an energy bandwidth for a single-shot x-ray emission spectrum of a few tens of eV.

Figure 2 shows the HEROS spectrum (black line) of Cu metal (Cu^0) recorded for 2000 XFEL shots with an incident beam energy of 8967 eV (i.e., 12 eV below the K ionization threshold, E_{initial}). The average pulse energy for the displayed spectrum was 0.9 mJ/shot. Any inherent variation in the number of incident photons influences uniformly the intensity of the measured HEROS spectrum (i.e., area of the measured spectrum), and not single data points. Thus, the HEROS spectra do not require any normalization procedures. As shown in Figure 2, the measured spectrum is characterized by a fast rise in intensity around 8036 eV when going from the high energy side to the low energy side. Following the fast rise in intensity, several resonances are detected at lower emission energies. The total fluorescence intensity then decreases by 50% over a 60 eV energy range.

To explain the shape of the HEROS spectrum and the origin of the detected structures, we performed calculations employing formulas developed by Tulkki and Åberg. In the case of off-resonant scattering around the Cu K-edge, the following equation was used to calculate the HEROS spectrum:

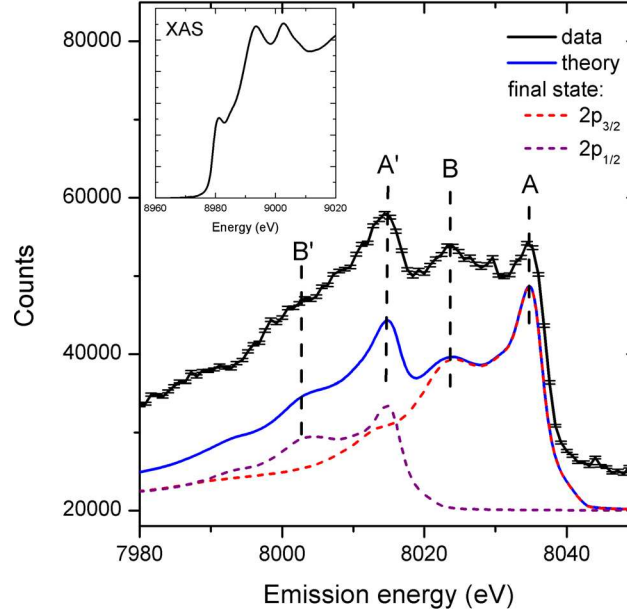


FIG. 2. HEROS spectra of Cu metal for 2000 self-seeded shots (black curve). The error bars represent the standard deviation of the total counts. For comparison, we plot the calculated spectrum using the Kramers-Heisenberg relation and a Cu K-edge XAS spectrum recorded at a synchrotron facility shown in inset (for more details see the text). The calculated curve represents the sum of two spectra relating to the final electronic states of $2p_{3/2}$ and $2p_{1/2}$.

$$XES(E_2) = \sum_{final=\frac{1}{2},\frac{3}{2}} \int_{E_1}^{E_2} \frac{E_2 (E_{initial} - E_{final})(E_{initial} + E) \cdot XAS(E)}{(E_{initial} + E - E_1)^2 + \Gamma_{initial}^2/4} \delta(E_1 - E_{final} - E - E_2) dE.$$

E_1 and E_2 are the energies of the incoming and emitted x-rays, respectively. $E_{initial}$ and E_{final} stand for energies of initial ($1s_{1/2}$) and final ($2p_{1/2,3/2}$) electronic states probed in the experiment. The natural lifetime of the initial state is represented by $\Gamma_{initial}$, and E stands for the energy of the photoelectron. The $XAS(E)$ function describes the p -projected density of unoccupied electronic states. Energies ($E_{initial}$ and E_{final}) and lifetime ($\Gamma_{initial}$) were taken from tabulated values,^{34,35} while for the $XAS(E)$ dependence we used a high energy resolution XAS spectrum of a Cu reference foil measured at a synchrotron facility (see Figure 2 inset). The computed curve is plotted in Figure 2 as a blue line together with the separate contributions of the final states (dashed lines). As shown, good agreement is obtained indicating that the same electronic states are probed with HEROS at an XFEL as with XAS at a synchrotron source. Following the XAS data interpretation in the literature,^{36,37} the resonances A and B relate to $1s \rightarrow 4p$ and multiple scattering of the photoelectron processes probed by the $2p_{3/2} \rightarrow 1s$ core-core electronic transition. The features A' and B' are sensitive to the same $1s$ electron excitation paths, however, probed by the $2p_{1/2} \rightarrow 1s$ decay channel. The second set of resonances are shifted down in energy according to the binding energy difference between the $2p_{1/2}$ and $2p_{3/2}$ states (i.e., 20 eV), as shown by dashed lines in Figure 2.

HEROS, as shown here, provides a complementary method for studying changes in the electronic structure induced by the chemical surrounding of the scattering atom at an XFEL. In order to test the capability of HEROS for chemical speciation, HEROS spectra for metallic Cu (Cu^0) and powder CuO (Cu^{2+}) were recorded, and are plotted in Figure 3. The HEROS spectra were acquired for 2000 (Cu) and 1000 (CuO) x-ray shots, at an incident beam energy of 8967 eV. As shown, relatively large spectral differences are observed due to the electronic structure difference of the Cu atom. The HEROS spectra are composed of two main contributions: the electronic structure of the unoccupied states and electronic structure of the final states. The chemical effects on final states are known to induce an energy shift of $2p_{3/2} \rightarrow 1s$ ($K\alpha_1$) and $2p_{1/2} \rightarrow 1s$ emission ($K\alpha_2$). For the off-resonant excitations, the strongest

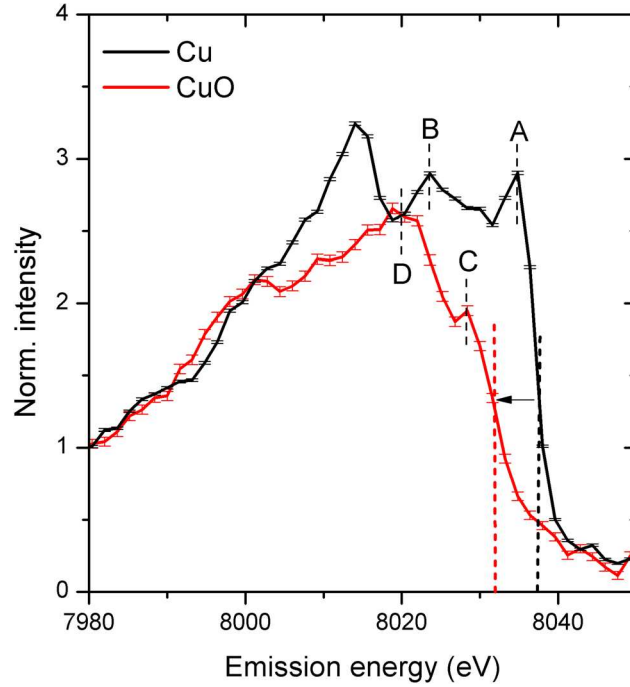


FIG. 3. HEROS spectra of Cu (black) and CuO (red) recorded for 2000 and 1000 XFEL pulses, respectively. For comparison, the spectra were normalized to 1 at an emission x-ray energy of 7980 eV. The origins of the marked resonances A, B, C, and D are discussed in the text.

contribution to the spectral shape is given by the unoccupied electronic states, which will shift in energy with the change from Cu^0 to Cu^{2+} . Therefore, the measured HEROS spectra are modulated mostly by the change in the unoccupied electronic structure, but are also slightly energy shifted by the final electronic state contribution. The origin of the resonances C and D in CuO are related to those observed in metallic Cu. Peak C corresponds to the $1s \rightarrow 4p$ dipole excitation, while the D resonance is described as multielectron scattering including shake-up processes to higher orbitals.^{37,38} The energy shift of the absorption edge of the HEROS spectrum between Cu and CuO samples (marked by an arrow) relates directly to the edge shift as observed in XAS. The energy position of the HEROS spectra edge ($E_{\text{cut-off}}$) is given by energy conservation principle and is expressed by

$$E_{\text{cut-off}} = E_1 + E_{\text{final} \rightarrow \text{initial}} - E_{\text{edge}}.$$

Therefore, the energy shift (ΔE) in HEROS spectra, measured at the same incident x-ray energy (E_1), is expressed by

$$\Delta E_{\text{cut-off}} = (E_{\text{Cu}} - E_{\text{CuO}})_{\text{final} \rightarrow \text{initial}} - (E_{\text{Cu}} - E_{\text{CuO}})_{\text{edge}}.$$

For the present experiment, we obtained $\Delta E_{\text{cut-off}}$ of -5 eV, a value close to the reported E_{edge} shift from synchrotron-based XAS spectra of -4.4 eV.³⁹ The difference of 0.6 eV may be attributed to the chemical shift of the $2p_{3/2} \rightarrow 1s$ transition.⁴⁰ These results show that single shot HEROS spectroscopy can provide detailed information about the electronic structure of matter at an XFEL, similar to how XAS provides information about the unoccupied electronic structure at synchrotrons. HEROS is equivalent to high resolution XAS, also called HERFD (“high energy resolution fluorescence detected”), in that the energy resolution of both techniques is limited only by the final state lifetime broadening, thus providing better resolution measurements than standard transmission or total fluorescence yield XAS. Both techniques have their advantages and disadvantages. High resolution XAS combined with focusing/scanning type

spectrometers provides higher count-rates and peak-to-background ratio. Therefore, it is best applied to dilute or low-concentration samples. On the other hand, the scanning-free capability of HEROS allows for spectroscopy measurements where the incident beam stability and/or tunability is an issue. Moreover, the fixed incident beam energy used for HEROS allows HEROS to be combined with other x-ray techniques such as diffraction or inelastic X-ray scattering.

The most important feature of XFEL sources is the delivery of very short and intense femtosecond x-ray pulses. To probe the capability of measuring electronic structure using a single femtosecond x-ray pulse, we analyzed the set of data for different numbers of pulses. The resulting spectra are plotted in Figure 4. Only the most intense pulses were considered, and the average energy was 0.9 mJ/pulse for the 2000 shots spectrum, 1.2 mJ/pulse for the 10 shots spectrum and 1.4 mJ/pulse for the single-shot spectrum. For comparison, the calculated HEROS signal from Figure 2 is shown by the dashed curve. Besides the decreasing signal-to-noise of the spectra with decreasing number of shots, all spectra exhibit the same structures and overall shape. The single-shot spectrum is of good enough quality to distinguish the rising edge and main electronic structures related to the $1s \rightarrow 4p$ excitation. This result indicates that the unoccupied electronic states may be probed using a single femtosecond x-ray pulse and that the recorded data quality is limited only by the number of incident x-rays and the efficiency of the detection setup. The addition of further crystal analyzers is a straightforward way to increase the efficiency of the detection setup.⁴¹ We would like to emphasize that the time resolution for detection is in principle limited only by the duration of the x-ray pulse. Therefore, HEROS may be applied as both the probe technique in a pump-probe configuration, as well as being used for measurements beyond the femtosecond limit when x-ray sources delivering shorter pulses will become available. The present HEROS experiment was performed on solid samples. When applied to less concentrated systems, for example a dilute protein sample in solution, the accumulation of a few tens to hundreds of x-rays shots may be necessary to obtain spectra of good quality. Because HEROS does not require normalization using the incident pulse energy, as opposed to a scanning measurement, this means that the only restriction is the availability of

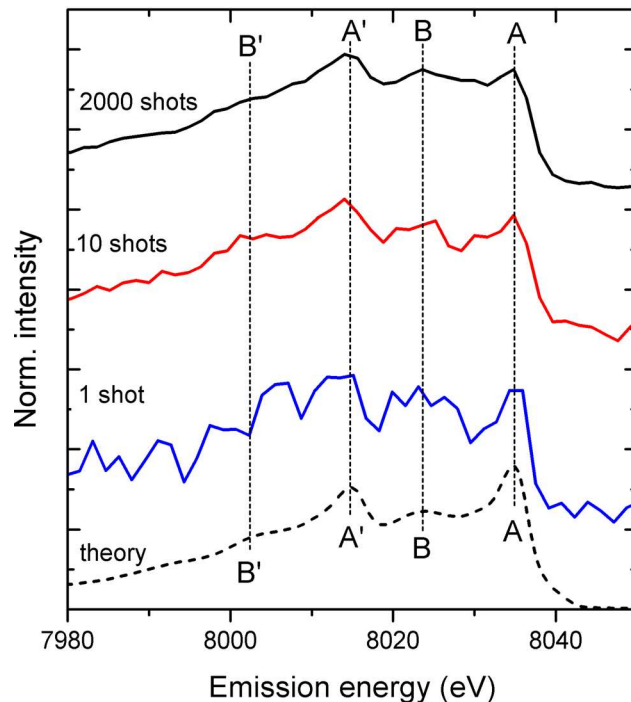


FIG. 4. HEROS spectra of Cu recorded for different number of shots. As shown, a 50 fs long X-ray pulse allows the main characteristic features (rising edge and resonance A) of the Cu electronic structure to be distinguished. For comparison, the calculated HEROS spectrum is plotted with a black dashed line. The marked features A, B, A', and B' are discussed in the text.

enough sample to obtain the desired signal-to-noise. Single-shot spectroscopy can, however, be performed on solid samples to study, for example, non-linear phenomena or plasma creation with strong x-ray pulses.

Recent progress in the development of advanced X-ray sources is devoted to understanding the fundamental processes arising in matter. Fourth-generation light sources, such as XFELs, produce intense femtosecond X-ray pulses that enable investigation of ultra-fast processes in matter. To advance the fundamental understanding of physical and chemical processes, new experimental techniques are required. We have demonstrated that high energy resolution off-resonant spectroscopy is capable of measuring unoccupied electronic density of state information with self-seeded femtosecond x-ray pulses. The HEROS spectra are derived at a single excitation energy and therefore corrections for the incident beam intensity fluctuations are not needed. Because the incoming and the measured photon energies are well below the absorption edge of the target atom, self-absorption processes do not affect the measured spectra. In other words, the derived HEROS spectra can be treated as measured. Finally, application of self-seeding XFEL operation leads to no pulse duration broadening caused by monochromator crystals.⁴² Temporal broadening of a short x-ray pulse relates to the extinction length of the x-rays into the monochromator crystal. For x-rays with a photon energy of a few keV, the extinction length amounts to few μm and may lead to pulse broadening of up to 20–30 fs.⁴³ In summary, HEROS provides a complementary technique to those already successfully implemented at XFELs, including x-ray diffraction, x-ray emission and x-ray absorption techniques.

We thank Eric De Boni for his help in the preparation, installation, and execution of the experiment. We would also like to thank Leonardo Sala for his help in organizing and implementing the data analysis tools at PSI. Finally, we would like to acknowledge the LCLS staff that helped implement the self-seeded beam for us. Some of us (J.H., J.-C.I.D., and W.B.) also acknowledge the financial support of the Swiss National Science Foundation.

¹B. W. J. McNeil and N. R. Thompson, *Nat. Photonics* **4**, 814 (2010).

²J. D. Brock, *Science* **315**, 609 (2007).

³K. J. Gaffney and H. N. Chapman, *Science* **316**, 1444 (2007).

⁴H. N. Chapman, P. Fromme, A. Barty, T. A. White, R. A. Kirian, A. Aquila, M. S. Hunter, J. Schulz, D. P. DePonte, U. Weierstall, R. B. Doak, F. R. N. C. Maia, A. V. Martin, I. Schlichting, L. Lomb, N. Coppola, R. L. Shoeman, S. W. Epp, R. Hartmann, D. Rolles, A. Rudenko, L. Foucar, N. Kimmel, G. Weidenspointner, P. Holl, M. Liang, M. Barthelmess, C. Caleman, S. Boutet, M. J. Bogan, J. Krzywinski, C. Bostedt, S. Bajt, L. Gumprecht, B. Rudek, B. Erk, C. Schmidt, A. Hömke, C. Reich, D. Pietschner, L. Strüder, G. Hauser, H. Gorke, J. Ullrich, S. Herrmann, G. Schaller, F. Schopper, H. Soltau, K.-U. Kühnel, M. Messerschmidt, J. D. Bozek, S. P. Hau-Riege, M. Frank, C. Y. Hampton, R. G. Sierra, D. Starodub, G. J. Williams, J. Hajdu, N. Timneanu, M. M. Seibert, J. Andreasson, A. Rocker, O. Jönsson, M. Svenda, S. Stern, K. Nass, R. Andritschke, C.-D. Schröter, F. Krasniqi, M. Bott, K. E. Schmidt, X. Wang, I. Grotjohann, J. M. Holton, T. R. M. Barends, R. Neutze, S. Marchesini, R. Fromme, S. Schorb, D. Rupp, M. Adolph, T. Gorkhober, I. Andersson, H. Hirsemann, G. Potdevin, H. Graafsma, B. Nilsson, and J. C. H. Spence, *Nature* **470**, 73 (2011).

⁵R. Bonifacio, L. De Salvo, P. Pierini, N. Piovella, and C. Pellegrini, *Phys. Rev. Lett.* **73**, 70 (1994).

⁶H. T. Lemke, C. Bressler, L. X. Chen, D. M. Fritz, K. J. Gaffney, A. Galler, W. Gawelda, K. Haldrup, R. W. Hartsock, H. Ihee, J. Kim, K. H. Kim, J. H. Lee, M. M. Nielsen, A. B. Stickrath, W. Zhang, D. Zhu, and M. Cammarata, *J. Phys. Chem. A* **117**, 735 (2013).

⁷G. Vankó, T. Neisius, G. Molnar, F. Renz, S. Karpati, A. Shukla, and F. M. F. de Groot, *J. Phys. Chem. B* **110**, 11647 (2006).

⁸P. Glatzel and U. Bergmann, *Coord. Chem. Rev.* **249**, 65 (2005).

⁹U. Bergmann and P. Glatzel, *Photosynth. Res.* **102**, 255 (2009).

¹⁰J. Kern, R. Alonso-Mori, R. Tran, J. Hattne, R. J. Gildea, N. Echols, C. Glockner, J. Hellmich, H. Laksmono, R. G. Sierra, B. Lassalle-Kaiser, S. Koroidov, A. Lampe, G. Han, S. Gul, D. DiFiore, D. Milathianaki, A. R. Fry, A. Miahnahri, D. W. Schafer, M. Messerschmidt, M. M. Seibert, J. E. Koglin, D. Sokaras, T. C. Weng, J. Sellberg, M. J. Latimer, R. W. Grosse-Kunstleve, P. H. Zwart, W. E. White, P. Glatzel, P. D. Adams, M. J. Bogan, G. J. Williams, S. Boutet, J. Messinger, A. Zouni, N. K. Sauter, V. K. Yachandra, U. Bergmann, and J. Yano, *Science* **340**, 491 (2013).

¹¹R. Alonso-Mori, J. Kern, R. J. Gildea, D. Sokaras, T. C. Weng, B. Lassalle-Kaiser, R. Tran, J. Hattne, H. Laksmono, J. Hellmich, C. Glockner, N. Echols, R. G. Sierra, D. W. Schafer, J. Sellberg, C. Kenney, R. Herbst, J. Pines, P. Hart, S. Herrmann, R. W. Grosse-Kunstleve, M. J. Latimer, A. R. Fry, M. M. Messerschmidt, A. Miahnahri, M. M. Seibert, P. H. Zwart, W. E. White, P. D. Adams, M. J. Bogan, S. Boutet, G. J. Williams, A. Zouni, J. Messinger, P. Glatzel, N. K. Sauter, V. K. Yachandra, J. Yano, and U. Bergmann, *Proc. Natl. Acad. Sci. U.S.A.* **109**, 19103–19107 (2012).

¹²L. Young, E. P. Kanter, B. Krässig, Y. Li, A. M. March, S. T. Pratt, R. Santra, S. H. Southworth, N. Rohringer, L. F. Dimauro, G. Doumy, C. A. Roedig, N. Berrah, L. Fang, M. Hoener, P. H. Bucksbaum, J. P. Cryan, S. Ghimire, J. M. Glowia, D. A. Reis, J. D. Bozek, C. Bostedt, and M. Messerschmidt, *Nature* **466**, 56 (2010).

¹³G. Doumy, C. Roedig, S. K. Son, C. I. Blaga, A. D. DiChiara, R. Santra, N. Berrah, C. Bostedt, J. D. Bozek, P. H. Bucksbaum, J. P. Cryan, L. Fang, S. Ghimire, J. M. Glowia, M. Hoener, E. P. Kanter, B. Krässig, M. Kuebel, M.

- Messerschmidt, G. G. Paulus, D. A. Reis, N. Rohringer, L. Young, P. Agostini, and L. F. Dimauro, *Phys. Rev. Lett.* **106**, 083002 (2011).
- ¹⁴J. Hozzowska, J. C. Dousse, J. Szlachetko, Y. Kayser, W. Cao, P. Jagodzinski, M. Kavčič, and S. H. Nowak, *Phys. Rev. Lett.* **107**, 053001 (2011).
- ¹⁵S. Pascarelli, O. Mathon, M. Munoz, T. Mairs, and J. Susini, *J. Synchrotron Radiat.* **13**, 351 (2006).
- ¹⁶M. Yabashi, J. B. Hastings, M. S. Zolotarev, H. Mimura, H. Yumoto, S. Matsuyama, K. Yamauchi, and T. Ishikawa, *Phys. Rev. Lett.* **97**, 084802 (2006).
- ¹⁷D. Zhu, M. Cammarata, J. M. Feldkamp, D. M. Fritz, J. B. Hastings, S. Lee, H. T. Lemke, A. Robert, J. L. Turner, and Y. Feng, *Appl. Phys. Lett.* **101**, 034103 (2012).
- ¹⁸J. Amann, W. Berg, V. Blank, F. J. Decker, Y. Ding, P. Emma, Y. Feng, J. Frisch, D. Fritz, J. Hastings, Z. Huang, J. Krzywinski, R. Lindberg, H. Loos, A. Lutman, H. D. Nuhn, D. Ratner, J. Rzepiela, D. Shu, Y. Shvyd'Ko, S. Spampinati, S. Stoupin, S. Terentyev, E. Trakhtenberg, D. Walz, J. Welch, J. Wu, A. Zholents, and D. Zhu, *Nat. Photonics* **6**, 693 (2012).
- ¹⁹P. Emma, R. Akre, J. Arthur, R. Bionta, C. Bostedt, J. Bozek, A. Brachmann, P. Bucksbaum, R. Coffee, F. J. Decker, Y. Ding, D. Dowell, S. Edstrom, A. Fisher, J. Frisch, S. Gilevich, J. Hastings, G. Hays, P. Hering, Z. Huang, R. Iverson, H. Loos, M. Messerschmidt, A. Miahnahri, S. Moeller, H. D. Nuhn, G. Pile, D. Ratner, J. Rzepiela, D. Schultz, T. Smith, P. Stefan, H. Tompkins, J. Turner, J. Welch, W. White, J. Wu, G. Yocky, and J. Galayda, *Nat. Photonics* **4**, 641 (2010).
- ²⁰T. Ishikawa, H. Aoyagi, T. Asaka, Y. Asano, N. Azumi, T. Bizen, H. Ego, K. Fukami, T. Fukui, Y. Furukawa, S. Goto, H. Hanaki, T. Hara, T. Hasegawa, T. Hatsui, A. Higashiya, T. Hirono, N. Hosoda, M. Ishii, T. Inagaki, Y. Inubushi, T. Itoga, Y. Joti, M. Kago, T. Kameshima, H. Kimura, Y. Kirihara, A. Kiyomichi, T. Kobayashi, C. Kondo, T. Kudo, H. Maesaka, X. M. Maréchal, T. Masuda, S. Matsubara, T. Matsumoto, T. Matsushita, S. Matsui, M. Nagasono, N. Nariyama, H. Ohashi, T. Ohata, T. Ohshima, S. Ono, Y. Otake, C. Saji, T. Sakurai, T. Sato, K. Sawada, T. Seike, K. Shirasawa, T. Sugimoto, S. Suzuki, S. Takahashi, H. Takebe, K. Takeshita, K. Tamasaku, H. Tanaka, R. Tanaka, T. Tanaka, T. Togashi, K. Togawa, A. Tokuhisa, H. Tomizawa, K. Tono, S. WU, M. Yabashi, M. Yamaga, A. Yamashita, K. Yanagida, C. Zhang, T. Shintake, H. Kitamura, and N. Kumagai, *Nat. Photonics* **6**, 540 (2012).
- ²¹T. Katayama, Y. Inubushi, Y. Obara, T. Sato, T. Togashi, K. Tono, T. Hatsui, T. Kameshima, A. Bhattacharya, Y. Ogi, N. Kurahashi, K. Misawa, T. Suzuki, and M. Yabashi, *Appl. Phys. Lett.* **103**, 131105 (2013).
- ²²J. Szlachetko, M. Nachttegaal, J. Sa, J.-C. Dousse, J. Hozzowska, E. Kleymenov, M. Janousch, O. V. Safonova, C. König, and J. A. van Bokhoven, *Chem. Commun.* **48**, 10898 (2012).
- ²³M. Kavčič, M. Žitnik, K. Bučar, A. Mihelič, B. Marolt, J. Szlachetko, P. Glatzel, and K. Kvashnina, *Phys. Rev. B* **87**, 075106 (2013).
- ²⁴H. A. Kramers and W. Heisenberg, *Z. Fur Phys.* **31**, 681 (1925).
- ²⁵J. Tulkki and T. Åberg, *J. Phys. B: At. Mol. Opt. Phys.* **15**, L435 (1982).
- ²⁶J. Tulkki, *Phys. Rev. A* **27**, 3375 (1983).
- ²⁷J. A. Carlisle, E. L. Shirley, E. A. Hudson, L. J. Terminello, T. A. Callcott, J. J. Jia, D. L. Ederer, R. C. C. Perera, and F. J. Himpsel, *Phys. Rev. Lett.* **74**, 1234 (1995).
- ²⁸H. Hayashi, Y. Udagawa, W. A. Caliebe, and C. C. Kao, *Chem. Phys. Lett.* **371**, 125 (2003).
- ²⁹J. Szlachetko, J. C. Dousse, J. Hozzowska, M. Pajek, R. Barrett, M. Berset, K. Fennane, A. Kubala-Kukus, and M. Szlachetko, *Phys. Rev. Lett.* **97**, 073001 (2006).
- ³⁰S. Boutet and G. J. Williams, *New J. Phys.* **12**, 035024 (2010).
- ³¹G. Geloni, V. Kocharyan, and E. Saldin, *J. Mod. Opt.* **58**, 1391 (2011).
- ³²J. Szlachetko, M. Nachttegaal, E. de Boni, M. Willmann, O. Safonova, J. Sa, G. Smolentsev, M. Szlachetko, J. A. van Bokhoven, J. C. Dousse, J. Hozzowska, Y. Kayser, P. Jagodzinski, A. Bergamaschi, B. Schmitt, C. David, and A. Lücke, *Rev. Sci. Instrum.* **83**, 103105 (2012).
- ³³S. Herrmann, S. Boutet, B. Duda, D. Fritz, G. Haller, P. Hart, R. Herbst, C. Kenney, H. Lemke, M. Messerschmidt, J. Pines, A. Robert, M. Sikorski, and G. Williams, *Nucl. Inst. Methods Phys. Res. A* **718**, 550–553 (2013).
- ³⁴R. D. Deslattes, E. G. Kessler, Jr., P. Indelicato, L. De Billy, E. Lindroth, and J. Anton, *Rev. Mod. Phys.* **75**, 35 (2003).
- ³⁵J. L. Campbell and T. Papp, *At. Data Nucl. Data Tables* **77**, 1 (2001).
- ³⁶G. N. Greaves, P. J. Durham, G. Diakun, and P. Quinn, *Nature* **294**, 139 (1981).
- ³⁷S. Bocharov, T. Kirchner, G. Dräger, O. Šipr, and A. Šimůnek, *Phys. Rev. B* **63**, 045104 (2001).
- ³⁸M. Calandra, J. P. Rueff, C. Gougoussis, D. Céolin, M. Gorgoi, S. Benedetti, P. Torelli, A. Shukla, D. Chandesris, and C. Brouder, *Phys. Rev. B* **86**, 165102 (2012).
- ³⁹L. A. Grunes, *Phys. Rev. B* **27**, 2111 (1983).
- ⁴⁰J. Kawai, Y. Nihei, M. Fujinami, Y. Higashi, S. Fukushima, and Y. Gohshi, *Solid State Commun.* **70**, 567 (1989).
- ⁴¹R. Alonso-Mori, J. Kern, D. Sokaras, T.-C. Weng, D. Nordlund, R. Tran, P. Montanez, J. Delor, V. K. Yachandra, J. Yano, and U. Bergmann, *Rev. Sci. Instrum.* **83**, 073114 (2012).
- ⁴²V. Bushuev, L. Samoylova, H. Sinn, and T. Tschentscher, *Proc. SPIE* **8141**, 81410T (2011).
- ⁴³S. D. Shastri, P. Zambianchi, and D. M. Mills, *J. Synchrotron Radiat.* **8**, 1131 (2001).